

**VALORIZATION OF ALGAL BIOMASS BY
EXTRACTING BIOACTIVE COMPOUNDS USING
SUPERCRITICAL CO₂ AND SUBCRITICAL
WATER EXTRACTION PROCESS**

NIDHI HANS



**CENTRE FOR RURAL DEVELOPMENT AND TECHNOLOGY
INDIAN INSTITUTE OF TECHNOLOGY DELHI**

JULY 2023

©Indian Institute of Technology Delhi (IITD), New Delhi, 2023

VALORIZATION OF ALGAL BIOMASS BY EXTRACTING BIOACTIVE COMPOUNDS USING SUPERCRITICAL CO₂ AND SUBCRITICAL WATER EXTRACTION PROCESS

by

NIDHI HANS

CENTRE FOR RURAL DEVELOPMENT AND TECHNOLOGY

Submitted

in fulfilment of the requirements of the degree of

Doctor of Philosophy

to the

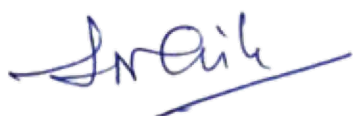


INDIAN INSTITUTE OF TECHNOLOGY DELHI

JULY 2023

CERTIFICATE

This is to certify that the thesis entitled “**Valorization of algal biomass by extracting bioactive compounds using supercritical CO₂ and subcritical water extraction process**”, being submitted by **Ms. Nidhi Hans** to the Indian Institute of Technology Delhi for the award of “**Doctor of Philosophy**” is a record of bonafide research work carried out by her. She has worked under our guidance and supervision and has fulfilled the requirements for the submission of this thesis. To the best of our knowledge, the results contained in this thesis have not been submitted in part or full to any other university or institute for the award of any degree or diploma.



Dr. Satya Narayan Naik
Professor (Emeritus)
Centre for Rural Development and
Technology
Indian Institute of Technology Delhi
New Delhi-110016



Dr. Anushree Malik
Professor
Centre for Rural Development and
Technology
Indian Institute of Technology Delhi
New Delhi-110016

Acknowledgments

Support and achievement go hand in hand. Without help, success is impossible. This has been my experience during the six years of my research. Quite a few individuals have provided me with intellectual and technical help, and now I have the opportunity to express my gratitude. Firstly, without the infinite kindness and love of the Almighty God, it would have been impossible to reach this milestone.

*It was an honor to work at the Centre for Rural Development and Technology (CRDT), Indian Institute of Technology Delhi. I would like to thank my supervisors **Prof. S. N. Naik** and **Prof. Anushree Malik** whose ample guidance, regular encouragement, and inspiration, I would not have been able to complete this work. Their tireless attitudes constantly encouraged me to work hard, and their availability and understanding, especially during pandemic, have been invaluable. Next, I would like to thank my SRC members, Prof. Satyawati Sharma, Prof. K. K. Pant, and Prof. J. K. Sahu, for providing insightful comments and valuable advice during my research. I would like to thank all the CRDT faculty members for their assistance in completing my thesis. I would also like to thank Prof. Ashok Kumar Patel and his research scholar, Ms. Shreya Gupta, from the Kusuma School of Biological Sciences for allowing us to utilize their laboratory and ensuring that our research was completed on time. I also acknowledge the contributions of CRF, NRF (IIT Delhi) and AIRF (JNU) for carrying out all the analysis.*

I would like to convey my heartfelt gratitude to Dr. Poonam Choudhary, Dr. Megha Mathur, and Dr. Farah Naaz for their kind support and invaluable suggestions during the early years of my PhD.

It is worth highlighting the names of two of my closest friends, Dr. Falguni Pattnaik and Dr. Shreya Tripathi, whose contributions are immeasurable. I express my sincere thanks Dr. Lopa Pattnaik, Dr. Ajay Patel, Dr. Smriti Kala, Dr. Chandrakant Sarkar, Mr. Gourav Choudhri, Ms. Vidhi Bhimjiyani, Mr. Bhushan Dole, Ms. Amreeta Preetam, Ms. Divya, Mr. Divyang Solanki, Ms. Tanya, and other students of IIT Delhi for all the help, advice, and pleasant company throughout. I would like to thank Mr. Abhishek Biswal, research scholar at SRM university for providing macroalgae samples. The utmost cooperation of office and lab staff, especially Mr. Mewa Lal, is sincerely acknowledged.

Finally, a heartfelt thanks to my parents, sisters, and brothers for all their love, care, encouragement and understanding throughout this journey. Without their blessings, it would not have been possible to venture this far. I would like to especially thank my husband, Mr. Arun Kumar M, for the moral support he has extended towards me in all the phases of my life.

Nidhi
Nidhi Hans

Abstract

The study depicts the use of various green extraction techniques including supercritical fluid extraction, ultrasound assisted extraction, enzyme assisted extraction and subcritical water extraction to utilize each fraction of an algal biomass for its conversion to value added products. In our research, we used the pilot scale algal biofilm reactor (100 L) to cultivate the microalgal consortia PA6 (*Chlorella* sp. and *Phormidium* sp.), and we procured red, green, and brown macroalgal biomass from the coasts of Tamil Nadu and Chilika lake, Orissa, India. The physicochemical characterization of biomass revealed that it contains high amount of carbohydrate ($\sim 20.4 \pm 0.5$ %), protein ($\sim 30 \pm 0.9$ %), fiber, dietary fiber, and minerals. The first step towards the valorization of algal biomass was extracting lipids using supercritical fluid extraction technique (SFE). The maximum lipid yield ($\sim 3 \pm 0.4$ %) was obtained by PA6 biomass which was found rich in polyunsaturated fatty acids content (20.68 %) with the presence of eicosapentaenoic acid, docosahexaenoic acid, α -linolenic acid, linoleic acid and arachidonic acid. The residual biomass after SFE showed recovery of 27.1 ± 0.9 mg g⁻¹ of total carotenoids, which could have applications in food industry.

The second stage of biomass valorization focuses on the polysaccharides contained in the SFE residual biomass. Using subcritical water (ScW) approach, ~ 14 % fucoidan and ~ 48 % of sodium alginate was recovered from SFE residual brown macroalgae. Furthermore, ultrasonication assisted approach recovered ~ 56 % of κ -carrageenan from SFE residual red macroalgae. Fucoidan and κ -carrageenan had sulfate content of 25 % and 28.5 %, respectively, which contributes to their biological activity. Analysis of monosaccharide composition of fucoidan reveals that ScW approach recovers highest content fucose (54.37 %) and galactose (83.32 %) with small amounts of arabinose, glucose, glucuronic acid, mannitol, mannose, rhamnose and xylose. The alginate derived from ScW revealed the presence of mannuronic (M) and guluronic acids (G) with M/G ratio greater than 1, fulfilling

WHO and FAO guidelines for the nutraceutical and pharmaceutical industries. κ -carrageenan exhibited a monosaccharide content of 3,6-anhydrogalactose (38.7 %) and galactose (23.1 %), as well as rheological properties within FAO limitations that can be explored for food-grade applications. In addition, it was shown that these extraction methods are selective for polyphenolic and flavonoid compounds, hence enhancing their antioxidant potential. These polysaccharides exhibited strong *invitro* 2,2-diphenyl-1-picrylhydrazyl scavenging activity (up to 88 %), 2,2'-azino-bis(3-ethylbenzothiazoline-6-sulfonic) acid radical scavenging activity (up to 80 %) and ferric reducing antioxidant power value. Hence, polysaccharides from macroalgae were recovered using environmentally friendly, sustainable methods with potential uses in the food, pharmaceutical, and cosmetics industries.

The final stage of biomass valorisation concentrates on the proteins present in the SFE residual biomass with the goal of producing a minimal quantity of waste by products. The protein yield in algal biomass using different pre-treatments including ultrasonication and homogenization varied from 0.1 mg g⁻¹ to 55.3 mg g⁻¹. *P. tetrastromatica* exhibited the maximum protein yield, therefore it was further optimised using ScW hydrolysis under various temperature and time conditions. The optimum conditions for obtaining the maximum protein (127.2 ± 1.1 mg g⁻¹), free amino acids (58.4 ± 1.0 mg g⁻¹), highest degree of hydrolysis (58.8 ± 1.2 %) and low molecular weight peptides (< 650 Da) were found to be 220 °C for 10 minutes. The amino acid profiling of the hydrolysate revealed that it contains 45 % essential amino acids, with the highest concentration of methionine (0.18 %), isoleucine (0.12 %) and leucine (0.10 %). It was found that the hydrolysate contains phenolics (23.9 ± 1.4 mg GAE g⁻¹) and flavonoids (1.23 ± 0.1 mg QE g⁻¹), which are largely responsible for antioxidant activity. The hydrolysate effectively inhibits acetylcholinesterase (up to 53 %) and α -amylase (up to 16 %) *invitro*, which can help in prevention of Alzheimer's disease and diabetes mellitus. Consequently, this study reveals that utilising eco-friendly subcritical water

hydrolysis method, ~ 79 % of protein was recovered from *P. tetrastromatica*, which might be an effective source as bioactive peptides in various nutraceutical, pharmaceutical and cosmeceutical applications.

In addition, the sulfated polysaccharides carrageenan and fucoidan extracted from red and brown macroalgae utilizing green emerging techniques were evaluated for their potential in inhibiting severe acute respiratory syndrome coronavirus 2 (SARS-CoV-2) by targeting its main protease (3CL^{pro}) and receptor binding domain (RBD) through *invitro* and *insilico* approach. According to the findings of our *invitro* study, κ -carrageenan from red macroalgae was effective in inhibiting the 3CL^{pro} of SARS-CoV-2 by up to 93 %, whereas fucoidan from brown macroalgae was effective in inhibiting the 3CL^{pro} of SARS-CoV-2 by up to 97 %. However, none of the sulfated polysaccharides were found to be active against the RBD protein. Molecular docking investigations of fucoidan revealed the lowest binding energy (-6.0 kcal mol⁻¹) for 3CL^{pro} compared to carrageenan (-5.2 kcal mol⁻¹). Molecular dynamics simulations results revealed that carrageenan and fucoidan successfully binds to the active site of the 3CL^{pro} while retaining the structural integrity and stability of protein-ligand complexes. The Absorption, Distribution, Metabolism, and Excretion (ADME) properties have been met by both compounds, although only fucoidan obeyed Lipinski's rule of five. The toxicity parameters suggested that neither of the compounds exhibit AMES toxicity, hepatotoxicity and skin sensitivity. Hence, carrageenan and fucoidan from macroalgae could act as possible inhibitors in regulating the function of the 3CL^{pro} protein, hence inhibiting viral replication and being effective against COVID 19.

Hence, the study brings out a promising pathway to valorize algal biomass by extracting multiple value-added compounds using green techniques for multiple industrial applications, thereby targeting a minimum waste generation approach. Besides, this study also highlights the limitations for practical implications at industrial scale. For this, a systematic study on

industrial scale cultivation and harvesting of algal biomass along with its life cycle assessment and techno-economic analysis is recommended to ensure recovery of similar types of industrially relevant food/pharma value products in a sustainable manner.

सारांश

अध्ययन में मूल्य वर्धित उत्पादों में इसके रूपांतरण के लिए शैवाल बायोमास के प्रत्येक अंश का उपयोग करने के लिए विभिन्न हरी निष्कर्षण तकनीकों के उपयोग को दर्शाया गया है। हमारे शोध में, हमने माइक्रोएलाल कंसोर्टिया PA6 (क्लोरेला एसपी. और फोर्मिडियम एसपी.) की खेती के लिए पायलट स्केल एलाल बायोफिल्म रिएक्टर (100 एल) का इस्तेमाल किया, और हमने तमिलनाडु और चिल्का झील, उड़ीसा, भारत के तटों से लाल, हरे और भूरे रंग के मैक्रोएलगल बायोमास की खरीद की। बायोमास के भौतिक-रासायनिक लक्षण वर्णन से पता चला है कि इसमें उच्च मात्रा में कार्बोहाइड्रेट ($\sim 20.4 \pm 0.5\%$), प्रोटीन ($\sim 30 \pm 0.9\%$), आहार फाइबर और खनिज शामिल हैं। अलाल बायोमास के मूल्यवर्धन की दिशा में पहला कदम सुपरक्रिटिकल द्रव निष्कर्षण तकनीक (एसएफई) का उपयोग करके लिपिड निकालना था। अधिकतम लिपिड उपज ($\sim 3 \pm 0.4\%$) PA6 बायोमास द्वारा प्राप्त किया गया था जो ईकोसापेन्टेनोइक एसिड, डोकोसाहेक्साएनोइक एसिड, α -लिनोलेनिक एसिड, लिनोलेनिक एसिड और एराचिडोनिक एसिड की उपस्थिति के साथ पॉलीअनसेचुरेटेड फैटी एसिड सामग्री (20.68%) में समृद्ध पाया गया था। एसएफई के बाद अवशिष्ट बायोमास ने कुल कैरोटेनॉयड्स के 27.1 ± 0.9 मिलीग्राम जी-1 की रिकवरी दिखाई, जिसका खाद्य उद्योग में अनुप्रयोग हो सकता है।

बायोमास वैलोराइजेशन का दूसरा चरण एसएफई अवशिष्ट बायोमास में निहित पॉलीसेकेराइड पर केंद्रित है। सबक्रिटिकल वाटर (ScW) दृष्टिकोण का उपयोग करते हुए, $\sim 14\%$ फ्यूकोइडान और $\sim 48\%$ सोडियम एल्गिनेट SFE अवशिष्ट ब्राउन मैक्रोलेगा से बरामद किया गया। इसके अलावा, अल्ट्रासोनिकेशन असिस्टेड एप्रोच ने एसएफई अवशिष्ट लाल मैक्रोलेगा से $\sim 56\%$ of-कैरेजेनन बरामद किया। Fucoidan और κ -carrageenan में क्रमशः 25% और 28.5% की सल्फेट सामग्री थी, जो उनकी जैविक गतिविधि में योगदान करती है। फ्यूकोइडान के मोनोसेकेराइड संरचना के विश्लेषण से पता चलता है कि ScW दृष्टिकोण उच्चतम सामग्री फ्यूकोस (54.37%) और गैलेक्टोज (83.32%) को कम मात्रा में अरबिनोज, ग्लूकोज, ग्लूकोरोनिक एसिड, मैनिटोल, मैनोज, रमनोज और ज़ाइलोज के साथ ठीक करता है। ScW से प्राप्त एल्गिनेट ने न्यूट्रास्यूटिकल और फार्मास्यूटिकल उद्योगों के लिए WHO और FAO दिशानिर्देशों को पूरा करते हुए 1 से अधिक M/G अनुपात के साथ मैन्यूरोनिक (M) और गुलुरोनिक एसिड (G) की उपस्थिति का खुलासा किया। κ -कैरेजेनन ने 3,6-

एनहाइड्रोगैलेक्टोज (38.7%) और गैलेक्टोज (23.1%) की एक मोनोसेकेराइड सामग्री के साथ-साथ एफएओ सीमाओं के भीतर रियोलॉजिकल गुण प्रदर्शित किए जिन्हें खाद्य-ग्रेड अनुप्रयोगों के लिए खोजा जा सकता है। इसके अलावा, यह दिखाया गया था कि ये निष्कर्षण विधियां पॉलीफेनोलिक और फ्लेवोनोइड यौगिकों के लिए चयनात्मक हैं, इसलिए उनकी एंटीऑक्सीडेंट क्षमता को बढ़ाती हैं। इन पॉलीसेकेराइड ने मजबूत इनविट्रो 2,2-डाइफेनिल-1-पिक्रीलहाइड्राज़ाइल सफाई गतिविधि (88% तक), 2,2'-एज़िनो-बीआईएस (3-एथिलबेनज़ोथियाज़ोलिन-6-सल्फ़ोनिक) एसिड कट्टरपंथी सफाई गतिविधि (80% तक) प्रदर्शित की और फेरिक एंटीऑक्सीडेंट पावर वैल्यू को कम करता है। इसलिए, भोजन, दवा और सौंदर्य प्रसाधन उद्योगों में संभावित उपयोग के साथ पर्यावरण के अनुकूल, टिकाऊ तरीकों का उपयोग करके मैक्रोलेगा से पॉलीसेकेराइड बरामद किए गए थे।

बायोमास वैलोराइजेशन का अंतिम चरण एसएफई अवशिष्ट बायोमास में मौजूद प्रोटीन पर ध्यान केंद्रित करता है, जिसमें उत्पादों द्वारा न्यूनतम मात्रा में अपशिष्ट का उत्पादन होता है। अल्बाल बायोमास में अल्ट्रासोनिकेशन और होमोजेनाइजेशन सहित विभिन्न पूर्व-उपचारों का उपयोग करके प्रोटीन की उपज 0.1 मिलीग्राम ग्राम⁻¹ से 55.3 मिलीग्राम ग्राम⁻¹ तक भिन्न होती है। पी. टेट्रास्ट्रोमैटिका ने अधिकतम प्रोटीन उपज का प्रदर्शन किया, इसलिए इसे विभिन्न दबाव और तापमान स्थितियों के तहत ScW हाइड्रोलिसिस का उपयोग करके और अधिक अनुकूलित किया गया। अधिकतम प्रोटीन (127.2 ± 1.1 मिलीग्राम ग्राम⁻¹), मुक्त अमीनो एसिड (58.4 ± 1.0 मिलीग्राम ग्राम⁻¹), हाइड्रोलिसिस की उच्चतम डिग्री (58.8 ± 1.2 %) और कम आणविक भार पेप्टाइड्स (<650 Da) प्राप्त करने के लिए इष्टतम स्थितियां 10 मिनट के लिए 220 डिग्री सेल्सियस पर पाया गया। हाइड्रोलाइज़ेट के अमीनो एसिड प्रोफाइलिंग से पता चला है कि इसमें मेथियोनिन (0.18%), आइसोल्यूसीन (0.12%) और ल्यूसीन (0.10%) की उच्चतम सांद्रता के साथ 45% आवश्यक अमीनो एसिड होते हैं। यह पाया गया कि हाइड्रोलाइज़ेट में फेनोलिक्स (23.9 ± 1.4 मिलीग्राम ग्राम⁻¹) और फ्लेवोनोइड्स (1.23 ± 0.1 मिलीग्राम क्यूई ग्राम⁻¹) शामिल हैं, जो एंटीऑक्सीडेंट गतिविधि के लिए काफी हद तक जिम्मेदार हैं। हाइड्रोलाइज़ेट क्रमशः 17.9 ± 0.1 मिलीग्राम मिलीलीटर⁻¹ और 16.0 ± 0.5 % के IC₅₀ मूल्यों के साथ इन विट्रो में एसिटाइलकोलिनेस्टरेज़ और अल्फा-एमिलेज़ को प्रभावी ढंग से रोकता है, जो अल्जाइमर रोग और मधुमेह मेलिटस की रोकथाम में मदद कर सकता है। नतीजतन, इस अध्ययन से पता चलता है कि पर्यावरण के अनुकूल

सबक्रिटिकल वॉटर हाइड्रोलिसिस विधि का उपयोग करते हुए, पी. टेट्रास्ट्रोमैटिका से 79% प्रोटीन बरामद किया गया, जो विभिन्न न्यूट्रास्यूटिकल, फार्मास्यूटिकल और कॉस्मिक््यूटिकल अनुप्रयोगों में बायोएक्टिव पेप्टाइड्स के रूप में एक प्रभावी स्रोत हो सकता है।

इसके अलावा, ग्रीन उभरती प्रौद्योगिकियों का उपयोग करते हुए लाल और भूरे रंग के मैक्रोलेगा से निकाले गए सल्फेटेड पॉलीसेकेराइड्स कैरेजेनन और फ्यूकोइडान का मूल्यांकन इसके मुख्य प्रोटीज (3CL^{pro}) और रिसेप्टर बाइंडिंग डोमेन (RBD) को लक्षित करके गंभीर तीव्र श्वसन सिंड्रोम कोरोनावायरस 2 (SARS-CoV-2) को इनविट्रो और इंसिलिको दृष्टिकोण के माध्यम से बाधित करने में उनकी क्षमता को देखा गया था। हमारे इनविट्रो अध्ययन के निष्कर्षों के अनुसार, लाल मैक्रोलेगा से κ -कैरेजेनन SARS-CoV-2 के 3CL^{pro} को 93 % तक बाधित करने में प्रभावी था, जबकि ब्राउन मैक्रोलेगा से फ्यूकोइडान SARS-CoV-2 के 3CL^{pro} को 97% तक बाधित करने में प्रभावी था। हालांकि, आरबीडी प्रोटीन के खिलाफ कोई भी सल्फेटेड पॉलीसेकेराइड निष्क्रिय नहीं पाया गया। फ्यूकोइडान की आणविक डॉकिंग (-6.0 kcal mol⁻¹) जांच से पता चला है कि कैरेजेनन (-5.2 किलो कैलोरी मोल⁻¹) की तुलना में 3CL^{pro} के लिए सबसे कम बाध्यकारी ऊर्जा है। आणविक गतिकी सिमुलेशन परिणामों से पता चला है कि प्रोटीन-लिगैंड परिसरों की संरचनात्मक अखंडता और स्थिरता को बनाए रखते हुए कैरेजेनन और फ्यूकोइडान सफलतापूर्वक 3CL^{pro} की सक्रिय साइट से जुड़ते हैं। अवशोषण, वितरण, चयापचय, और उत्सर्जन (एडीएमई) गुण दोनों यौगिकों द्वारा मिले हैं, हालांकि केवल फ्यूकोइडान ने लिपिंस्की के पांच के नियम का पालन किया। विषाक्तता पैरामीटर बताते हैं कि यौगिकों में से कोई भी एएमईएस विषाक्तता, हेपेटॉक्सिसिटी और त्वचा संवेदनशीलता प्रदर्शित नहीं करता है। इसलिए, मैक्रोलेगा से कैरेजेनन और फ्यूकोइडान 3CL^{pro} प्रोटीन के कार्य को विनियमित करने में संभावित अवरोधक के रूप में कार्य कर सकते हैं, इसलिए वायरल प्रतिकृति को रोकते हैं और COVID 19 के खिलाफ प्रभावी होते हैं।

इसलिए, अध्ययन कई औद्योगिक अनुप्रयोगों के लिए हरित प्रौद्योगिकियों का उपयोग करके एक आशाजनक मार्ग सामने लाता है, जिससे न्यूनतम अपशिष्ट उत्पादन दृष्टिकोण को लक्षित किया जाता है। इसके अलावा, अध्ययन औद्योगिक पैमाने पर व्यावहारिक प्रभाव की सीमाओं पर भी प्रकाश डालता है। इसके लिए, समान प्रकार के औद्योगिक रूप से प्रासंगिक खाद्य/फार्मा वैल्यू उत्पादों की सतत तरीके से रिकवरी सुनिश्चित करने के

लिए, इसके जीवन चक्र मूल्यांकन और तकनीकी-आर्थिक विश्लेषण के साथ-साथ शैवाल बायोमास की औद्योगिक पैमाने पर खेती और कटाई पर एक व्यवस्थित अध्ययन की सिफारिश की जाती है।

TABLE OF CONTENTS

Certificate		i
Acknowledgments		ii
Abstract		iv
Table of contents		xii
List of Figures		xviii
List of Tables		xxi
List of Abbreviations		xxiii
List of Symbols		xxv
Chapter 1: Introduction		
1.1	General Background	1
1.2	Worldwide production of algae	1
1.3	Marine derived bioactive compounds	3
	1.3.1 Lipids	3
	1.3.2 Proteins, peptides and amino acids	4
	1.3.3 Pigments	5
	1.3.3.1 Chlorophyll	6
	1.3.3.2 Carotenoids	6
	1.3.4 Polysaccharides and dietary fiber	9
	1.3.5 Phenolic compounds	11
	1.3.6 Vitamins	12
	1.3.7 Minerals	12
1.4	Extraction techniques	13
	1.4.1 Conventional extraction	13
	1.4.2 Modern extraction techniques	14
	1.4.2.1 Supercritical fluid extraction	14
	1.4.2.2 Subcritical water extraction	16
	1.4.2.3 Ultrasound assisted extraction	18
	1.4.2.4 Microwave assisted extraction	18
	1.4.2.5 Enzyme assisted extraction	20
Chapter 2: Literature review		
2.1	Marine derived bioactive compounds	23
2.2	Extraction of lipids from algal biomass	28
2.3	Extraction of polysaccharides from algal biomass	32
2.4	Extraction of proteins from macroalgal biomass	38
2.5	Biological activity of algal derived sulfated polysaccharides	40
2.6	Scope of the work	44
2.7	Objectives	46
Chapter 3: Physiochemical characterization of algal biomass through proximate, ultimate and compositional analysis		
3.1	Materials and methods	47
	3.1.1 Mass cultivation and harvesting of biomass	47
	3.1.2 Proximate analysis	50

	3.1.3	Elemental analysis	50
	3.1.4	Mineral analysis	50
	3.1.5	Thermogravimetric analysis (TGA) of biomass	51
	3.1.6	Fourier-transform infrared spectroscopy (FTIR)	51
	3.1.7	Total carbohydrate content	51
	3.1.8	Fiber analysis	52
	3.1.9	Total dietary fiber (TDF) of the biomass	53
	3.1.10	Determination of total phenolic content of biomass extract	55
	3.1.11	Determination of total flavonoid content of biomass extract	55
	3.1.12	Statistical analysis	56
3.2	Results and discussion		56
	3.2.1	Physicochemical analysis of biomass	56
	3.2.2	Mineral analysis of biomass	59
	3.2.3	TGA analysis of the biomass	61
	3.2.4	FTIR analysis of biomass	61
	3.2.5	Analysis of total carbohydrate content in the biomass	64
	3.2.6	Analysis of fiber and dietary fiber of biomass	65
	3.2.7	Phenolic and flavonoid content of the biomass	66
3.3	Summary		68
Chapter 4: Effect of different parameters on polyunsaturated fatty acids recovered from algal biomass using supercritical fluid technique			
4.1	Materials and methods		69
	4.1.1	Solvent extraction of lipids from biomass	69
	4.1.2	Supercritical fluid extraction of lipids from biomass	70
	4.1.3	Fatty acid methyl esterification of extracted lipids	70
	4.1.4	Fatty acid profiling using gas chromatography mass spectrometry	71
	4.1.5	Extraction of carotenoids from SFE residual biomass	71
	4.1.6	Analysis of carotenoids using high performance liquid chromatography	72
4.2	Result and discussion		73
	4.2.1	Analysis of lipid yield from micro- and macro- algae using SFE and solvent method	73
	4.2.2	Fatty acid profiling of extracted lipids	75
	4.2.3	Analysis of carotenoids from SFE residual biomass	79
4.3	Summary		82
Chapter 5: Extraction, characterization and biological activity of fucoidan from SFE residual brown macroalgae			
5.1	Materials and methods		84
	5.1.1	Extraction of fucoidan from <i>Padina tetrastratica</i> and <i>Turbinaria conoides</i>	84
	5.1.2	Estimation of sulfate content in fucoidan	85
	5.1.3	Spectral analysis of extracted fucoidan	86
	5.1.3.1	Fourier transform-infrared spectroscopy	86

		5.1.3.2	Fourier transform-near infrared spectroscopy	86
		5.1.3.3	Proton and Two-Dimensional Nuclear Magnetic Resonance spectroscopy	86
	5.1.4	Monosaccharide composition of fucoidan by high pressure liquid chromatography		86
	5.1.5	Bioactive assay of fucoidan		87
		5.1.5.1	Total phenolic content	87
		5.1.5.2	Total flavonoid content	87
		5.1.5.3	2,2-diphenyl-1-picrylhydrazyl radical scavenging assay	88
		5.1.5.4	2,2'-azino-bis(3-ethylbenzothiazoline-6-sulfonic) acid radical scavenging assay	88
		5.1.5.5	Ferric reducing antioxidant power assay	89
	5.1.6	Scanning electron microscopy of leftover biomass and fucoidan		90
	5.1.7	Statistical analysis		90
5.2	Results and discussion			90
	5.2.1	Analysis of fucoidan yield from convention and modern technologies		90
	5.2.2	Analysis of sulfate content in fucoidan		92
	5.2.3	Analysis of FTIR and FT-NIR spectroscopy of fucoidan		94
	5.2.4	Analysis of ¹ H and 2D NMR of fucoidan		97
	5.2.5	Analysis of monosaccharide composition of fucoidan		99
	5.2.6	Total phenolic and flavonoid content in <i>P. tetrastromatica</i> and <i>T. conoides</i> extracts		101
	5.2.7	<i>Invitro</i> antioxidant activity of fucoidan		103
	5.2.8	Analysis of scanning electron microscopy		107
5.3	Summary			109
Chapter 6: Extraction and characterization of sodium alginate polysaccharide from SFE residual brown macroalgae				
6.1	Materials and Methods			110
	6.1.1	Extraction and purification of sodium alginate from SFE residual biomass		110
	6.1.2	Structural characterization using spectroscopy		111
		6.1.2.1	Fourier transform-infrared spectroscopy	111
		6.1.2.2	Proton nuclear magnetic resonance spectroscopy	111
	6.1.3	Monosaccharide composition by high pressure liquid chromatography		112
	6.1.4	Bioactivity of sodium alginate		112
		6.1.4.1	Total phenolic content of sodium alginate	112
		6.1.4.2	Total flavonoid content of sodium alginate	112
		6.1.4.3	<i>Invitro</i> antioxidant activity by 2,2-diphenyl-1-picrylhydrazyl assay	112
		6.1.4.4	2,2'-azino-bis(3-ethylbenzothiazoline-6-sulfonic) acid radical scavenging assay	112
	6.1.5	Scanning electron microscopy analysis residual biomass		112

	6.1.6	Statistical analysis	113
6.2	Results and Discussion		113
	6.2.1	Effect of extraction techniques on yield of sodium alginate	113
	6.2.2	FTIR analysis of sodium alginate	115
	6.2.3	¹ H-NMR analysis of sodium alginate	116
	6.2.4	Monosaccharide composition of sodium alginate	118
	6.2.5	Phenolic and flavonoid content of sodium alginate	119
	6.2.6	<i>Invitro</i> antioxidant activity of sodium alginate	122
	6.2.7	Morphological analysis of SFE and ScW residual biomass	124
6.3	Summary		126
Chapter 7: Extraction and characterization of κ-carrageenan polysaccharide from SFE residual red macroalgae			
7.1	Material and Methods		128
	7.1.1	Extraction of κ -carrageenan from SFE residual biomass	128
	7.1.2	Analysis of sulfate content	130
	7.1.3	Structural characterization using spectroscopy	130
		7.1.3.1	Fourier transform-infrared spectroscopy
		7.1.3.2	¹³ C solid nuclear magnetic resonance (NMR) spectroscopy
	7.1.4	Monosaccharide composition of κ -carrageenan by HPLC	131
	7.1.5	Flow behaviour and viscoelastic characterization of κ -carrageenan	131
	7.1.6	Residual biomass analysis	131
	7.1.7	Statistical analysis	132
7.2	Results and Discussion		132
	7.2.1	Analysis of κ -carrageenan yield	132
	7.2.2	Sulfate content analysis of κ -carrageenan	133
	7.2.3	Structural analysis of κ -carrageenan by FTIR spectroscopy	134
	7.2.4	Structural analysis of κ -carrageenan by solid NMR spectroscopy	136
	7.2.5	Monosaccharide composition analysis of κ -carrageenan	138
	7.2.6	Analysis of rheological behaviour of κ -carrageenan	139
	7.2.7	SEM analysis of residual biomass	142
7.3	Practical applications of κ -carrageenan		143
7.4	Summary		144
Chapter 8: Subcritical water hydrolysis of SFE residual algal biomass for the extraction of protein			
8.1	Materials and methods		145
	8.1.1	Extraction of protein from SFE residual algal biomass	145
	8.1.2	Subcritical water hydrolysis (ScW) process	146
	8.1.3	Estimation of total protein content, total free amino acids, pH, and colour of the hydrolysate	147
	8.1.4	Degree of hydrolysis	148
	8.1.5	Amino acid profiling of biomass and ScW hydrolysate	149

	8.1.6	Estimation of reducing sugars by Dintrosalicylic Acid colorimetric method	149
	8.1.7	Estimation of total phenolic content by Folin-Ciocalteu assay	150
	8.1.8	Estimation of total flavonoid content by aluminium chloride method	150
	8.1.9	Evaluation of <i>invitro</i> antioxidant capacity of hydrolysate	150
	8.1.9.1	2,2-diphenyl-1-picrylhydrazyl radical scavenging assay	150
	8.1.9.2	2,2'-azino-bis(3-ethylbenzothiazoline-6-sulfonic) acid radical scavenging assay	150
	8.1.9.3	Ferric reducing antioxidant power assay	150
	8.1.10	Enzyme inhibition assay of ScW hydrolysate	150
	8.1.10.1	<i>Invitro</i> acetylcholinesterase inhibition assay	150
	8.1.10.2	<i>Invitro</i> α -amylase inhibition assay	151
	8.1.11	Functional properties of ScW hydrolysate	152
	8.1.11.1	Foaming and stability capacity of hydrolysate	152
	8.1.11.2	Turbidity of the hydrolysate	152
	8.1.12	Analysis of residue biomass	152
	8.1.13	Statistical analysis	153
8.2	Result and discussion		153
	8.2.1	Effect of different pretreatments on protein yield	153
	8.2.2	Effect of temperature and time on protein yield and free amino acids	154
	8.2.3	Effect of temperature and time on pH and colour of ScW hydrolysate	157
	8.2.4	Degree of hydrolysis	160
	8.2.5	Amino acid analysis of biomass and ScW hydrolysate	163
	8.2.6	Effect of temperature and time on total reducing sugar of hydrolysate	165
	8.2.7	Effect of temperature and time on phenolic and flavonoid content	166
	8.2.8	Effect of temperature on antioxidant activity of ScW hydrolysate	169
	8.2.9	Effect of temperature and time on <i>invitro</i> acetylcholinesterase inhibition effect	172
	8.2.10	Effect of temperature and time on <i>invitro</i> α -amylase inhibition effect	173
	8.2.11	Effect of temperature on Foaming and stability capacity of the hydrolysate	174
	8.2.12	Effect of temperature on Turbidity of the hydrolysate	175
	8.2.13	Residual biomass analysis	178
	8.2.13.1	SEM analysis	178
	8.2.13.2	Elemental analysis	179
	8.2.13.3	XRD analysis	180
8.3	Summary		181
Chapter 9: <i>Invitro</i> and <i>insilico</i> analysis of antiviral activity of sulfated polysaccharide from macroalgae			
9.1	Material and Methods		184
	9.1.1	Cloning and expression of 3CL ^{pro} and RBD protein	184
	9.1.2	Preparation of sulfated polysaccharide extract	185

	9.1.3	Evaluation of protease inhibition activity using casein substrate	185
	9.1.4	<i>Insilico</i> investigation of the molecular interactions between sulfated polysaccharide and 3CL ^{pro}	186
	9.1.4.1	Ligand selection and protein structure preparation	186
	9.1.4.2	Preparation of protein and grid parameters using molecular docking	186
	9.1.4.3	Molecular dynamics simulations of protein- sulfated polysaccharide complex	187
	9.1.4.4	MMPBSA binding free energy calculation of protein-ligand interaction	188
	9.1.4.5	Drug-likeness, pharmacokinetics, and toxicity parameters of ligand molecule	190
	9.1.5	Statistical analysis	191
9.2	Result and Discussion		191
	9.2.1	Inhibition of 3CL ^{pro} activity by sulfated polysaccharide	191
	9.2.2	Inhibition of RBD enzyme activity by sulfated polysaccharide	193
	9.2.3	Analysis of molecular docking interaction of sulfated polysaccharide against main protease of SARS-CoV-2	196
	9.2.4	Analysis of molecular dynamics simulations and stability of protein-ligand complex	197
	9.2.4.1	Root mean square deviation analysis	198
	9.2.4.2	Root mean square fluctuation analysis	198
	9.2.4.3	Radius of gyration analysis	199
	9.2.4.4	Solvent accessible surface area analysis	199
	9.2.4.5	Hydrogen bond number and hydrogen number distribution analysis	199
	9.2.5	Analysis of free binding energies by MMPBSA calculation	202
	9.2.6	Analysis of drug-like properties of carrageenan and fucoidan	203
9.3	Summary		205
Chapter 10: Summary and Conclusions			
10.1	Under-utilized algal biomass with high bioactive compounds		206
10.2	Suitable extraction technique to isolate lipids		207
10.3	Valorization of SFE residual biomass for separation of polysaccharides		207
10.4	Process optimization for extraction of protein from SFE residual biomass		208
10.5	Assessment of the therapeutic potential of sulfated polysaccharides		209
10.6	Benefits of the study and scope of the future research		210
References			213
List of Publications			248
Biodata			252

LIST OF FIGURES

Figure 1.1	Schematic representation of Supercritical CO ₂ apparatus (a) and phase diagram of CO ₂	15
Figure 1.2	Schematic representation of subcritical water apparatus (a) and phase diagram of water	17
Figure 2.1	Chemical structure of marine derived sulfated polysaccharides	36
Figure 3.1	Image of microalgal consortium PA6 (a), <i>Kappaphycus alvarezii</i> (b), <i>Gelidiella acerosa</i> (c), <i>Gracilaria verrucosa</i> (d), <i>Halimeda gracilis</i> (e), <i>Padina tetrostromatica</i> (e) and <i>Turbinaria conoides</i> (f) biomass	49
Figure 3.2	Thermogravimetric analysis of algal biomass	62
Figure 3.3	Fourier-transform infrared spectroscopy analysis of algal biomass	63
Figure 5.1	Comparison of fucoidan yield from <i>P. tetrastromatica</i> and <i>T. conoides</i> using conventional and modern technologies	92
Figure 5.2	Sulfate content analysis in fucoidan extracted from <i>P. tetrastromatica</i> and <i>T. conoides</i> using various technologies	94
Figure 5.3	FT-IR (a) and FT-NIR (b) spectroscopy of fucoidan extracted using different methods	96
Figure 5.4	(a) ¹ H NMR and 2D ¹ H COSY spectra of Fucoidan extracted from <i>Padina tetrostromatica</i> using ScW (b) ¹ H NMR and 2D ¹ H COSY spectra of Fucoidan extracted from <i>Turbinaria conoides</i> using ScW (c) Fucoidan structure	98
Figure 5.5	Monosaccharide composition (%) of fucoidan from <i>P. tetrastromatica</i> (a) and <i>T. conoides</i> (b) using different extraction methods	100
Figure 5.6	Total phenolic content (a) and total flavonoid content (b) in fucoidan extract from <i>P. tetrastromatica</i> and <i>T. conoides</i> using different extraction methods	102
Figure 5.7	<i>Invitro</i> antioxidant activity (a) DPPH (b) ABTS (c) FRAP of fucoidan extracted using different techniques	105
Figure 5.8	Microscopic structure of (i) untreated biomass (ii) aqueous (iii) EAE (iv) UAE (v) ScW (vi) fucoidan from (A) <i>P. tetrastromatica</i> and (B) <i>T. conoides</i>	108
Figure 6.1	Comparative sodium alginate yield from <i>P. tetrastromatica</i> and <i>T. conoides</i> using different extraction techniques	114
Figure 6.2	FTIR spectroscopy of sodium alginate extracted from (a) <i>P. tetrastromatica</i> (b) <i>T. conoides</i> using different methods	116
Figure 6.3	¹ H NMR spectra of sodium alginate extracted from <i>P. tetrastromatica</i> using ScW extraction method (b) ¹ H NMR spectra of sodium alginate extracted from <i>T. conoides</i> using ScW method (c) Sodium alginate structure	118
Figure 6.4	(a) Total phenolic content of sodium alginate from <i>P. tetrastromatica</i> and <i>T. conoides</i> (b) total flavonoid content of sodium alginate from <i>P. tetrastromatica</i> and <i>T. conoides</i> using different extraction techniques	120
Figure 6.5	<i>Invitro</i> DPPH (a,b) and ABTS (c,d) scavenging activity of sodium alginate from <i>P. tetrastromatica</i> and <i>T. conoides</i> , respectively extracted using various technologies	124
Figure 6.6	Surface morphology of untreated, SFE and ScW residual biomass of <i>P. tetrastromatica</i> (a) and <i>T. conoides</i> (b)	125
Figure 7.1	Steps involved in extraction of carrageenan and its purification from	130

	<i>Kappaphycus alvarezii</i>	
Figure 7.2	Comparative κ -carrageenan yield from <i>K. alvarezii</i> using different extraction techniques	133
Figure 7.3	Sulfate content of κ -carrageenan extracted from <i>K. alvarezii</i> using different techniques	134
Figure 7.4	FTIR spectra of the (a) parent biomass and the carrageenan extracted from the biomass through (b) aqueous extraction in alkaline medium (c) aqueous extraction in neutral medium (d) KOH treatment (e) homogenization (f) ultrasonication (g) enzymatic treatment	135
Figure 7.5	Solid C13 NMR spectra of κ -carrageenan extracted from <i>Kappaphycus alvarezii</i> using ultrasonic assisted extraction	137
Figure 7.6	Rheological characteristics of κ -carrageenan extracted using different methods (a) shear rate v/s dynamic viscosity κ -carrageenan (b) shear strain amplitude sweep test with variation in storage modulus (G') and loss modulus (G'') (c) Frequency dependence of G' and G'' of κ -carrageenan	141
Figure 7.7	Scanning electron microscopy (SEM) images of <i>K. alvarezii</i> after different treatments (a) untreated biomass (b) SFE residual biomass (c) UAE residual biomass (d) ScW hydrolysis residual biomass	143
Figure 8.1	Comparative protein extraction yields algal biomass in SFE residual biomass after different pretreatment processes	154
Figure 8.2	Total protein content (a) and total free amino acids (b) in ScW hydrolysate of <i>P. tetrastromatica</i>	157
Figure 8.3	pH values at different temperature and time during ScW hydrolysis process of <i>P. tetrastromatica</i>	158
Figure 8.4	Colour parameters (A) L (lightness) value (B) a^* (redness) value (C) b^* (yellowness) value of ScW hydrolysate	159
Figure 8.5	Degree of hydrolysis (a) and molecular weight distribution (b) of ScW hydrolysate of <i>P. tetrastromatica</i> at different temperature and time conditions	161
Figure 8.6	Total reducing sugar (a), total phenolic content (b), total flavonoid content (c) of ScW hydrolysate of <i>P. tetrastromatica</i>	168
Figure 8.7	Invitro antioxidant activity (a) DPPH (b) ABTS (c) FRAP of ScW hydrolysate of <i>P. tetrastromatica</i> at different temperature	171
Figure 8.8	Acetylcholinesterase (AChE) enzyme inhibitory activity of ScW hydrolysate from <i>P. tetrastromatica</i>	173
Figure 8.9	SEM analysis (a) untreated biomass (b) ScW hydrolysis residual biomass at 100 °C (c) ScW hydrolysis residual biomass at 220 °C	179
Figure 8.10	XRD of raw and residual biomass after ScW hydrolysis at 220 °C	181
Figure 9.1	(A) Binding of ligand (green) and protein (red) in presence of solvent (blue) gives ΔG_{bind} free binding energy (B) Thermodynamic cycle involved in the estimation of the free binding energy of protein-ligand complexes, where $\Delta G_{\text{solv,ligand}}$ is difference in binding energy of ligand in presence and absent of solvent (vacuum), $\Delta G_{\text{solv,receptor}}$ is difference in binding energy of protein in presence and absent of solvent, $\Delta G_{\text{bind,solvent}}$ is binding energy of protein and ligand in solvent, $\Delta G_{\text{bind,vacuum}}$ is binding energy of protein and ligand in vacuum and $\Delta G_{\text{solv,complex}}$ is difference in binding energy of protein-ligand complex in presence and absent of solvent	190

Figure 9.2	3CL ^{pro} inhibition activity of sulfated polysaccharides (A) carrageenan from <i>Kappaphycus alvarezii</i> (B) fucoidan from <i>Padina tetrostromatica</i> and <i>Turbanaria conoides</i> using casein as substrate	193
Figure 9.3	RBD inhibition activity of sulfated polysaccharides (A) control (B) carrageenan from <i>Kappaphycus alvarezii</i> (B) fucoidan from <i>Padina tetrostromatica</i> and <i>Turbanaria conoides</i>	194
Figure 9.4	Molecular docking 2D docking representation between active site of 3CL ^{pro} and (a) carrageenan (b) fucoidan	197
Figure 9.5	Analysis of molecular dynamics simulations and stability of protein-ligand complex: (a) root mean square deviation (RMSD) backbone (b) root mean square fluctuation (RMSF), (c) radius of gyration (Rg), (d) solvent accessible surface area (SASA) (e) hydrogen bond numbers (f) hydrogen bond distribution of carrageenan and fucoidan binding to the 3CL ^{pro} during MD simulation	201
Figure 10.1	Biorefinery approach of biomass by extracting multiple value-added compounds using sequential green extraction techniques	212

LIST OF TABLES

Table 1.1	Strengths and drawbacks of conventional and modern techniques for the extraction of bioactive compounds	21
Table 2.1	Marine algae derived bioactive compounds, their sources, health benefits and applications	25
Table 2.2	Extraction of lipids from few microalgae and macroalgae using different extraction approaches	29
Table 2.3	Extraction of polysaccharides from macroalgae	37
Table 2.4	Extraction of protein from different biomass feedstock using subcritical water hydrolysis process	39
Table 2.5	Antiviral activity of some sulfated polysaccharides from marine algae	43
Table 3.1	Elemental analysis, moisture content, ash content and volatile matter of micro- and macro- algal biomass	58
Table 3.2	Mineral analysis of micro- and macro- algal biomass using ICP-MS	60
Table 3.3	Assignments of the different bands obtained by the FTIR analysis of the algal biomass	64
Table 3.4	Total carbohydrate, dietary fiber, phenolic and flavonoid content of micro- and macro- algal biomass	67
Table 4.1	Comparison of lipid yield using supercritical CO ₂ and solvent extraction method	75
Table 4.2	Retention time (minutes) and peak area (%) of compounds present in lipids extracted from microalgae (PA6) using solvent and SFE method	77
Table 4.3	Retention time (minutes) and peak area (%) of compounds present in lipids extracted from <i>Kappaphycus alvarezii</i> , <i>Padina tetrastromatica</i> and <i>Turbinaria conoides</i> using solvent (hexane) and SFE method	80
Table 4.4	Comparison of total carotenoid yield from raw and SFE residual biomass	81
Table 5.1	Monosaccharide composition percentage of fucoidan from <i>P. tetrastromatica</i> and <i>T. conoides</i> using different extraction methods	101
Table 5.2	Total phenolic, total flavonoid, and IC ₅₀ of DPPH, ABTS, FRAP of fucoidan extracted from <i>P. tetrastromatica</i> and <i>T. conoides</i> using different techniques	106
Table 6.1	Structural characterization of sodium alginate extracted from <i>P. tetrastromatica</i> and <i>T. conoides</i>	117
Table 6.2	Effect of different extraction methods on yield, monosaccharide composition, phenolic content, flavonoid content and antioxidant activity of sodium alginate extracted from <i>P. tetrastromatica</i> and <i>T. conoides</i>	121
Table 7.1	Assignments of the different bands obtained by the FTIR analysis of the κ-carrageenan	136
Table 7.2	Monosaccharide composition (%) of carrageenan extracted from <i>K. alvarezii</i> using different methods	139
Table 8.1	Effect of temperature and time on Protein yield, TFAA, pH, colour and degree of hydrolysis of ScW hydrolysate	162
Table 8.2	Amino acid profiling of <i>P. tetrastromatica</i> and its ScW hydrolysate obtained at 220 °C	164
Table 8.3	Total phenolic content, total flavonoid content, total reducing sugar content, DPPH, ABTS, FRAP, enzyme inhibition activity of ScW	176

	hydrolysate extracted from <i>P. tetrastromatica</i>	
Table 8.4	Elemental analysis of <i>P. tetrastromatica</i> (raw) and residual biomass after ScW hydrolysis	180
Table 9.1	Average value of root mean square deviation backbone (RMSD), RMSD ligand, root mean square fluctuation (RMSF), the radius of gyration (Rg), solvent accessible surface area (SASA) of carrageenan-3CLpro complex and fucoidan 3CLpro complex during molecular dynamics simulation	200
Table 9.2	Physicochemical properties, water solubility, lipophilicity, pharmacokinetics, druglikeness and toxicity of carrageenan and fucoidan	204

LIST OF ABBREVIATIONS

CO ₂ - Carbon dioxide	UAE- Ultrasound assisted extraction
FAO- Food and Agriculture Organization	EAE- Enzyme assisted extraction
PUFAs- Polyunsaturated fatty acids	SPs- Sulfated polysaccharides
hACE- Human angiotensin-converting enzyme	ICPMS- Inductively Coupled Plasma Mass Spectrometry
DHA- Docosahexaenoic acid	TGA- Thermogravimetric analysis
GLA- Gamma-linolenic acids	IC ₅₀ : Half-maximal inhibitory concentration
AA- Arachidonic acid	NDF- Neutral detergent fibre
EPA- Eicosapentaenoic acid	ADF- Acid detergent fibre
MAA- Mycosporine-like amino acids	ADL- Acid detergent lignin
EFSA- European food safety authority	ANOVA- Analysis of variance
U.V- ultraviolet	BHT- Butylated hydroxy toluene
DNA- Deoxyribonucleic acid	DNSA- 3,5-dinitrosalicylic acid
RNA- Ribonucleic acid	DPPH- 2,2-Diphenyl-1-picrylhydrazyl
ROS- Reactive oxygen species	SEM- Scanning electron microscope
HIV- Human immunodeficiency virus	TDF- Total dietary fiber
SFE- Supercritical fluid	IDF- Insoluble dietary fiber
PA6- <i>Chlorella</i> sp. and <i>Phormidium</i> sp.	SDF- soluble dietary fiber
GRAS- Generally regarded as safe	GAE- Gallic acid equivalent
FDA- Food Drug and Administration	QE- Quercetin equivalent
ScW- Subcritical water	FAME- fatty acid methyl esters
NREL- National Renewable Energy laboratory	MBTH- 3-methyl-2-benzothiazolinone hydrazone hydrochloride-assay
CHNS- Carbon, hydrogen, nitrogen and sulphur	¹ H NMR- Proton nuclear magnetic resonance spectroscopy (NMR)
HPLC- High-performance liquid chromatography	FTIR- Fourier transform infrared spectroscopy
VAPs- Value added products	MUFAs- Monounsaturated fatty acids
NIR- Near Infrared	SFAs- Saturated fatty acids
GCMS- Gas chromatography-mass spectrometry	ABTS- 2,2'-azino-bis(3-ethylbenzothiazoline-6-sulfonic) acid

RID- Refractive index detector	OPA- o-phthalaldehyde
FRAP- Ferric reducing antioxidant power	TCA- Trichloroacetic acid
¹³ C- Carbon nuclear magnetic resonance	BHA- Butylated hydroxyanisole
2D ¹ H COSY- Two-dimensional proton COrrrelation SpectroscopY	M/G- β-D-mannuronic acid/ α-L-guluronic acid
HAE- Homogenization assisted extraction	G'- Storage modulus
G''- Loss modulus	WHO- World Health Organization
RT- Retention time	LVR- Linear viscoelastic region
TFAA- Total free amino acid	DH- Degree of hydrolysis
SARS-CoV-2- Severe acute respiratory syndrome coronavirus 2	SDS-PAGE- Sodium dodecyl sulfate- polyacrylamide gel electrophoresis
AChE- Acetylcholineesterase	XRD- X-ray diffraction
TRS- Total reducing sugar	PDB- Protein Data Bank
3CL ^{pro} - 3-chymotrypsin like protease	RBD- Receptor binding domain
DTT- Dithiothreitol	PMSF- Phenylmethylsulfonyl fluoride
BME- Beta mercaptoethanol	COVID-19- Coronavirus disease 19
MD simulations- Molecular dynamics simulations	RCSB- Research Collaboratory for Structural Bioinformatics
BE- Binding energy	GROMACS- GRONingen MACHine for Chemical Simulations
RMSD- Root mean square deviation	RMSF- Root mean square fluctuation
Rg- Radius of gyration	SASA- solvent accessible surface area
MMPBSA - Molecular Mechanic/Poisson- Bolt-Boltzmann Surface Area	ADME- Absorption, distribution, metabolism and excretion

LIST OF SYMBOLS

KHz, MHz, GHz- Kilo, Mega and Giga Hertz	NaOH- Sodium hydroxide
°C- Degree centigrade	Mg – milligram
HCl- Hydrochloric acid	%- Percentage
MPa- Megapascal	v/v- volume by volume
Na ₂ CO ₃ - Sodium carbonate	w/v- weight by volume
Min- Minutes	wt.%- Weight percentage
h- Hours	R ² - Co-efficient of determination or regression
W- Watt	Ca(OH) ₂ - Calcium hydroxide
KOH- Potassium hydroxide	KCl- Potassium chloride
Rpm- Revolutions per minute	Pa s- Pascal second
rad sec ⁻¹ - Radian per second	kDa- Kilo Dalton
AlCl ₃ - Aluminium chloride	A.U- Absorbance unit
mM- milli molar	KJ mol ⁻¹ - Kilojoules per mole
K- Kelvin	Å - Armstrong
H ₂ SO ₄ - Sulphuric acid	